ACS APPLIED MATERIALS & INTERFACES

Letter

www.acsami.org

Strongly Improved Electrochemical Cycling Durability by Adding Iridium to Electrochromic Nickel Oxide Films

Rui-Tao Wen,* Gunnar A. Niklasson, and Claes G. Granqvist

The Ångström Laboratory, Department of Engineering Sciences, Uppsala University, P.O. Box 534, SE-75121 Uppsala, Sweden

ABSTRACT: Anodically colored nickel oxide (NiO) thin films are of much interest as counter electrodes in tungsten oxide based electrochromic devices such as "smart windows" for energy-efficient buildings. However, NiO films are prone to suffering severe charge density degradation upon prolonged electrochemical cycling, which can lead to insufficient device lifetime. Therefore, a means to improve the durability of NiO-based films is an important challenge at present. Here we report that the incorporation of a modest amount of iridium into NiO films [Ir/(Ir + Ni) = 7.6 atom %] leads to remarkable durability, exceeding 10000 cycles in a lithium-conducting electrolyte, along with significantly improved optical modulation during extended cycling. Structure characterization showed that the face-centered-cubic-type NiO structure remained after iridium addition. Moreover, the crystallinity of these films was enhanced upon electrochemical cycling.

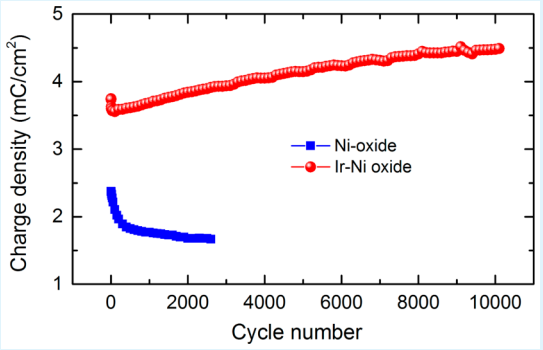

KEYWORDS: *electrochromic, iridium−nickel oxide, improved durability, charge density, optical modulation*

Electrochromic thin-film devices are of much current interest for "smart windows" capable of varying their throughput of visible light and solar energy so that buildings can be rendered both energy-efficient and comfortable.[1−3] These devices normally utilize joint transport of small ions and electrons between a thin film of tungsten oxide (WO_3) and a counter electrode based on nickel oxide (NiO), basically in the same way as in an electrical battery, and the optical transmittance is low when the charge resides in WO_3, while the transmittance is high when the charge is in NiO. NiO films suffer from optical degradation and limitation in modulation span under extended electrochemical cycling,[4−6] and several recent studies aimed at alleviating these deficiencies have been reported. Beneficial effects of additives to NiO have been studied, specifically for litihum,[7,8] carbon,[9,10] nitrogen,[11] tungsten,[12] (Li,W),[13] (Li,Al),[14] (Li,Zr),[15] and several more. Nevertheless, the most crucial problem for NiO-based films, viz., their cycling durability, is still far from solved. In a previous paper,[4] we showed that degradation of the charge density in NiO follows a power-law decay model upon cycling in 1 M $LiClO_4$ dissolved in propylene carbonate (Li−PC), and long-term degradation, hence, not only curtails the cycle life but also gradually erodes the optical modulation span of the device. In this Letter, we report that the charge density exchange in NiO-based thin films can be significantly *increased* during extended electrochemical cycling if the films contain a modest amount of iridium, and optical modulation is concomitantly enhanced.

We deposited IrO−NiO films by cosputtering from metallic iridium and nickel targets in an argon−oxygen atmosphere onto unheated glass coated with In_2O_3:Sn (i.e., ITO, 60 Ω/□). Films were also prepared on carbon substrates for composition determination. The film thickness t was determined by surface profilometry across a step edge. The iridium content in NiO was characterized by Rutherford backscattering spectroscopy (RBS). Figure 1a shows RBS spectra of pristine NiO and IrO−NiO films and indicates that the iridium is homogeneously distributed over the film's cross section. Fitting the experimental data by use of the *SIMNRA* program[16] yielded Ir/(Ir + Ni) = 7.6 atom %. The film density was 5.6 g/cm^3. X-ray diffraction (XRD) patterns demonstrated that IrO−NiO films have the same face-centered-cubic (fcc) structure as NiO (JCPDS no. 04-0385), as seen from Figure 1b. No diffraction peaks from IrO_2 or iridium were observed; rutile IrO_2 and metallic iridium would have yielded features at 28.1° and 34.7° and at 40.1°, respectively. From the (200) diffraction peak, the grain size was estimated to be 13 and 21 nm for IrO−NiO and NiO, respectively. Expanded diffraction features in the 34−48° region revealed that peaks due to the (111) and (200) reflections shifted somewhat toward lower angles by iridium incorporation, thus indicating enlarged d spacing. Correspondingly, the cell volume for IrO−NiO is also slightly greater than that of NiO. This enlargement is in line with the expected structural variation when Ir atoms (radius = 0.180 nm) replace Ni atoms (0.149 nm)[17] and may facilitate charge exchange as discussed later.

We performed cyclic voltammetry (CV) measurements between 2.0 and 4.1 V versus Li/Li$^+$ in 1 M Li−PC. In situ optical transmittance data in the wavelength (λ) range 380−800 nm

Received: February 24, 2015
Accepted: April 28, 2015
Published: April 28, 2015

DOI: 10.1021/acsami.5b01715
ACS Appl. Mater. Interfaces 2015, 7, 9319−9322

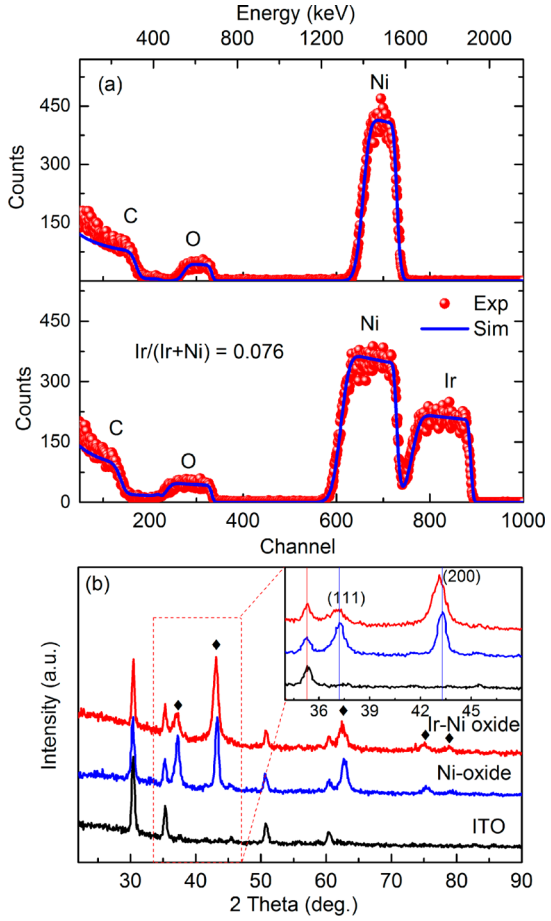

Figure 1. (a) Experimental and simulated RBS spectra for as-deposited thin films of NiO ($t \approx 180$ nm) and IrO–NiO ($t \approx 270$ nm) on carbon substrates. The measurement used 2 MeV ^{4}He ions backscattered at an angle of 170°. Red dots are experimental results, and blue lines are simulated spectra. (b) XRD characterization of NiO and IrO–NiO films. Data for ITO are presented for comparison. Diffraction peaks agree well with the standard pattern of cubic NiO, as indicated by black diamonds. The inset is a close-up view of the 34–48° region. Vertical blue lines serve as guides for the eye. The vertical red line in the inset indicates that the peak due to ITO diffraction did not change. Data were taken by use of a Siemens D5000 instrument operating with Cu K_α radiation at a wavelength of 0.0154 nm.

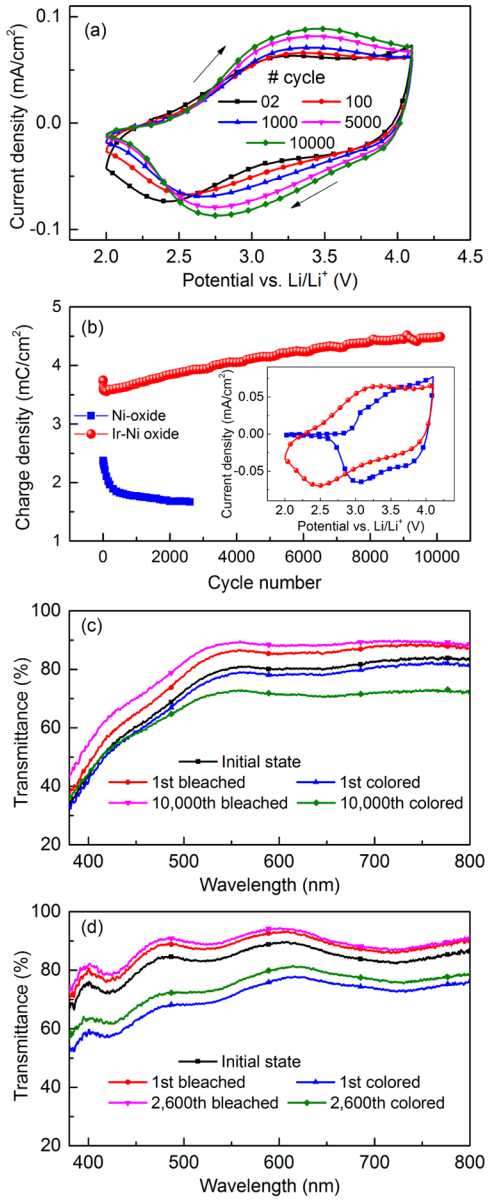

Figure 2. (a) Cyclic voltammograms for a thin film of IrO–NiO ($t \approx 300$ nm) in 1 M Li–PC taken after the indicated number of cycles. The voltage sweep rate was 50 mV/s, and the arrows indicate the sweep direction. (b) Charge density as a function of the cycle number for the IrO–NiO film and also for NiO ($t \approx 250$ nm) in the voltage range 2.0–4.1 V versus Li/Li$^+$ at 50 mV/s. The inset shows CV curves for the corresponding films after five CV cycles. (c and d) Optical transmittance spectra for IrO–NiO and NiO before and after 10000 and 2600 CV cycles, respectively.

were used to simultaneously record optical spectra before and after CV recordings. Figure 2a displays examples of cyclic voltammograms for an IrO–NiO film for up to 10000 cycles. It is evident that both anodic and cathodic peak currents increase substantially as cycling progresses. By integrating the inserted and extracted charge from the CV curves, it was found that the charge density grew monotonically for increasing cycle number, apart from in the first few cycles (Figure 2b). This unexpected behavior points at extreme cycling durability for the IrO–NiO film. For the NiO film, CV data taken for 2600 cycles were sufficient to reveal a strong loss of the charge density (Figure 2b). The open-circuit potential for IrO–NiO was 3.13 V initially and increased to 3.25 V versus Li/Li$^+$ after 10000 cycles. In NiO, this potential was 3.17 V initially and decreased to 3.09 V versus Li/Li$^+$ after 2600 cycles.

The charge density for IrO–NiO is obviously larger than that for NiO (Figure 2b), although the film thicknesses are similar. The larger cell volume, associated with the increased d spacing, is one reason that may facilitate charge exchange. However, the main reason lies in the different charge insertion and extraction processes. Specifically, most charge insertion and extraction take place between 2.7 and 4.1 V versus Li/Li$^+$ for pure NiO (Figure 2b, inset), whereas insertion and extraction occur in the entire 2.0–4.1 V versus Li/Li$^+$ range for IrO–NiO, as it also does for pure IrO.[18] Thus, we surmise that the increased charge density in the latter film is due to a contribution from iridium occurring primarily below 2.7 V. Enhanced charge density becomes even more pronounced for still larger iridium contents in the films (not shown). Optical transmittance spectra revealed that optical modulation ($T_{bleached} - T_{colored}$) for IrO–NiO is significantly enhancd from the initial 7.5% (at $\lambda = 550$ nm) to

DOI: 10.1021/acsami.5b01715
ACS Appl. Mater. Interfaces 2015, 7, 9319–9322

16.5% at the 10000th cycle (Figure 2c), which is due to its increased charge density exchange upon cycling. It is also seen that optical modulation of the IrO−NiO film is somewhat smaller than that of a comparable NiO film (Figure 2d), especially at short wavelengths, where the introduction of iridium appears to introduce some extra absorption. Hence, the coloration efficiency for the IrO−NiO film is also smaller than that for the NiO film, even after 10000 cycles, because of the smaller optical modulation and larger charge density.

Scanning electron microscopy (SEM) was used to study possible morphological changes upon charge exchange between the IrO−NiO film and electrolyte. The SEM image exhibits a pristine film comprising small grains and cracks (Figure 3a).

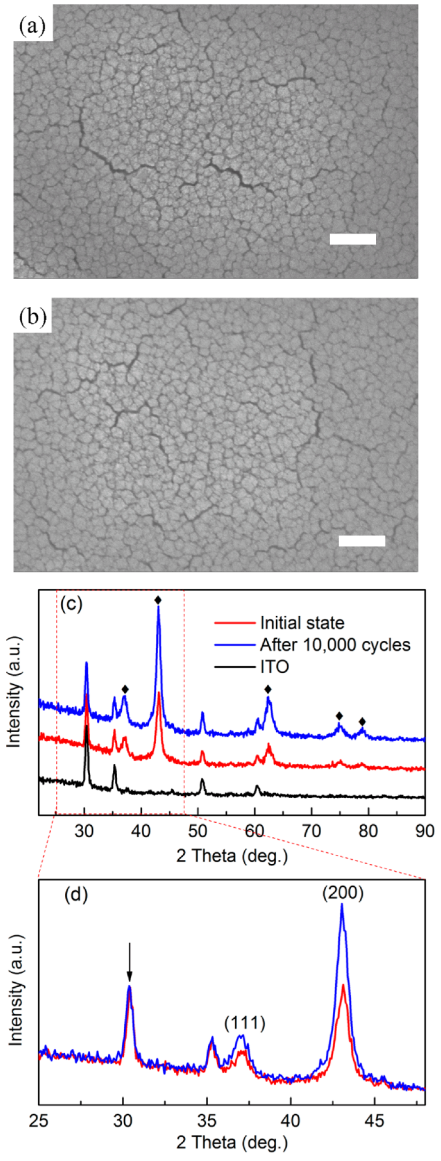

Figure 3. SEM images of an IrO−NiO thin film (a) before and (b) after electrochemical cycling for 10000 times between 2.0 and 4.1 V versus Li/Li^+. Data were recorded by use of a LEO 1550 FEG Gemini instrument with an acceleration voltage of 10 kV. The scale bars are 200 nm. (c) XRD pattern for an IrO−NiO film before and after 10000 CV cycles and (d) a close-up view for the 25−48° range. Intensity curves (in arbitrary units, au) are vertically displaced in part c. The blue arrow at ∼30.4° in part d indicates that the ITO peak has the same diffraction intensity before and after cycling.

After 10000 CV cycles, the morphology looks much the same (Figure 3b), which confirms that the surface structure is stable. XRD data taken after 10000 cycles showed that the film still exhibited the same fcc structure as that in the initial state (Figure 3c). Using the (200) peak, the grain size was calculated from Scherrer's formula[19] to be ∼13 nm for the film both before and after CV cycling. A detailed comparison of the diffraction features revealed that the peak intensities for the IrO−NiO film became noticeably more distinct after electrochemical cycling, whereas the ITO-based features remained almost the same. We have at present no explanation for this unexpected result.

In summary, we have demonstrated that charge density exchange, optical modulation, and crystallinity improve in IrO−NiO thin films subjected to extended electrochemical cycling in a Li^+-conducting electrolyte, whereas no similar effects are present in the absence of iridium. The significance of these results is that IrO−NiO thin films can yield a highly stable and reversible electrochromic effect upon charge exchange and can serve as an excellent anode in WO_3-based electrochromic devices. Further work is needed to ascertain the optimum Ir content for electrochromics-based applications.

AUTHOR INFORMATION

Corresponding Author

*E-mail: Ruitao.Wen@angstrom.uu.se.

Notes

The authors declare no competing financial interest.

ACKNOWLEDGMENTS

We acknowledge support with RBS measurements from Daniel Primetzhofer and the staff of the Tandem Accelerator Laboratory at Uppsala University. Financial support was received from the European Research Council under the European Community's Seventh Framework Program (FP7/2007-2013)/ERC Grant 267234 ("GRINDOOR").

REFERENCES

(1) Granqvist, C. G. *Handbook of Inorganic Electrochromic Materials*; Elsevier: Amsterdam, The Netherlands, 1995.

(2) Gillaspie, D. T.; Tenent, R. C.; Dillon, A. C. Metal-oxide Films for Electrochromic Applications: Present Technology and Future Directions. *J. Mater. Chem.* **2010**, *20*, 9585−9592.

(3) Granqvist, C. G. Electrochromics for Smart Windows: Oxide-based Thin Films and Devices. *Thin Solid Films* **2014**, *564*, 1−38.

(4) Wen, R.-T.; Granqvist, C. G.; Niklasson, G. A. Cyclic Voltammetry on Sputter-deposited Films of Electrochromic Ni oxide: Power-law Decay of the Charge Density Exchange. *Appl. Phys. Lett.* **2014**, *105*, 163502.

(5) Wen, R.-T.; Niklasson, G. A.; Granqvist, C. G. Electrochromic Nickel Oxide Films and Their Compatibility with Potassium Hydroxide and Lithium Perchlorate in Propylene Carbonate: Optical, Electrochemical and Stress-related Properties. *Thin Solid Films* **2014**, *565*, 128−135.

(6) Bouessay, I.; Rougier, A.; Poizot, P.; Moscovici, J.; Michalowicz, A.; Tarascon, J. M. Electrochromic Degradation in Nickel Oxide Thin Film: A Self-discharge and Dissolution Phenomenon. *Electrochim. Acta* **2005**, *50*, 3737−3745.

(7) Kubo, T.; Nishikitani, Y.; Sawai, Y.; Iwanaga, H.; Sato, Y.; Shigesato, Y. Electrochromic Properties of Li_xNi_yO Films Deposited by RF Magnetron Sputtering. *J. Electrochem. Soc.* **2009**, *156*, H629−H633.

(8) Tenent, R. C.; Gillaspie, D. T.; Miedaner, A.; Parilla, P. A.; Curtis, C. J.; Dillon, A. Fast-switching Electrochromic Li^+-doped NiO Films

DOI: 10.1021/acsami.5b01715
ACS Appl. Mater. Interfaces 2015, 7, 9319−9322

by Ultrasonic Spray Deposition. *J. Electrochem. Soc.* **2010**, *157*, H318−H322.
(9) Lin, Y.-S.; Lin, D.-J.; Sung, P.-J.; Tien, S.-W. Atmospheric-pressure Plasma-enhanced Chemical Vapour Deposition of Electrochromic Organonickel Oxide Thin Films with an Atmospheric Pressure Plasma Jet. *Thin Solid Films* **2013**, *532*, 36−43.
(10) Lin, Y.-S.; Lin, D.-J.; Chiu, L.-Y.; Lin, S.-W. Lithium Electrochromism of Atmospheric Pressure Plasma Jet-synthesized NiO_xC_y Thin Films. *J. Solid State Electrochem.* **2013**, *16*, 2581−2590.
(11) Lin, F.; Gillaspie, D. T.; Dillon, A. C.; Richards, R. M.; Engtrakul, C. Nitrogen-doped Nickel Oxide Thin Films for Enhanced Electrochromic Applications. *Thin Solid Films* **2013**, *527*, 26−30.
(12) Green, S. V.; Granqvist, C. G.; Niklasson, G. A. Structure and Optical Properties of Electrochromic Tungsten-containing Nickel Oxide. *Sol. Energy Mater. Sol. Cells* **2014**, *126*, 248−259.
(13) Gillaspie, D.; Norman, A.; Tracy, C. E.; Pitts, J. R.; Lee, S.-H.; Dillon, A. Nanocomposite Counter Electrode Materials for Electrochromic Windows. *J. Electrochem. Soc.* **2010**, *157*, H328−H331.
(14) Lin, F.; Nordlund, D.; Weng, T. C.; Moore, R. G.; Gillaspie, D. T.; Dillon, A.; Richards, R. M.; Engtrakul, C. Hole Doping in Al-containing Nickel Oxide Materials to Improve Electrochromic Performance. *ACS Appl. Mater. Interfaces* **2013**, *5*, 301−309.
(15) Lin, F.; Nordlund, D.; Weng, T. C.; Sokaras, D.; Jones, K. M.; Reed, R. B.; Gillaspie, D. T.; Weir, D. G. J.; Moore, R. G.; Dillon, A.; Richards, R. M.; Engtrakul, C. Origin of Electrochromism in High-performing Nanocomposite Nickel Oxide. *ACS Appl. Mater. Interfaces* **2013**, *5*, 3643−3649.
(16) Mayer, M. SIMNRA, A Simulation Program for the Analysis of NRA, RBS and ERDA. *Am. Inst. Phys. Conf. Proc.* **1999**, *475*, 541−544.
(17) Clementi, E.; Raimondi, D. L. Atomic Screening Constants from SCF Functions. *J. Chem. Phys.* **1963**, *38*, 2686−2689.
(18) Wen, R.-T.; Niklasson, G. A.; Granqvist, C. G. Electrochromic Iridium Oxide Films: Compatibility with Propionic Acid, Potassium Hydroxide, and Lithium Perchlorate in Propylene Carbonate. *Sol. Energy Mater. Sol. Cells* **2014**, *120*, 151−156.
(19) Cullity, B. D.; Stock, S. R. *Elements of X-ray Diffraction*, 3rd ed.; Prentice-Hall: Upper Saddle River, NJ, 2001.

DOI: 10.1021/acsami.5b01715
ACS Appl. Mater. Interfaces 2015, 7, 9319−9322